THE GEOLOGICAL SOCIETY OF AMERICA®

Addressing time-scale–dependent erosion rates from measurement methods with censorship

Brandon McElroy[1,†], Jane Willenbring[2], and David Mohrig[3]

[1]*Department of Geology & Geophysics, University of Wyoming, 1000 E. University Avenue, Laramie, Wyoming 82071, USA*

[2]*Scripps Institution of Oceanography–Earth Division, University of California–San Diego, 9500 Gilman Drive, La Jolla, California 92093, USA*

[3]*Department of Geological Sciences, University of Texas, 1 University Station C9000, Austin, Texas 78712, USA*

ABSTRACT

In a degrading landscape, does the episodic nature of erosion affect observed erosion rates in a systematic way, and can one account for the effects? We present a null hypothesis for surface change rate variations based on minimal assumptions about the processes of topographic evolution. Variance in erosion along with censorship of topographic change distributions combine to act as a first-order control on time-scale dependence of erosion rates. In general, censorship is ubiquitous, and as a result, time-scale dependence of rates is likely to apply to almost every system. In detail, this occurs because at short time scales, surface changes can be censored from field measurements that become inherently incorporated by natural surface evolution at longer time scales. Additionally, the granularity of systems implies minimum time scales below which specific rate measurements have no physical interpretation. Finally, we show the existence of a crossover time scale at which the short-term rate dependence of a process gives way to the long-term rate that is no longer subject to censoring.

We demonstrate these points by applying the proposed framework to a growing seepage channel network in Florida, United States. Using a dendrogeomorphic approach in concert with cosmogenic radionuclide methods, we estimate denudation rates averaged over annual to multimillennial time scales. Exposure of hundreds of tree roots combined with tree ages supplies surface change rates along approximately one third of the valley bottom within the studied area. Erosion rates are distributed approximately between 1 mm/yr and 10 mm/yr. This erosion exhibits variance that depends linearly on time scale and is interpreted to represent a process well modeled as normal diffusion. As a result, the erosion rates show an inverse-square dependence on time scale. We used the ^{10}Be contents from nine quartz sand samples to estimate long-term erosion rates and then coupled them with existing estimates of long-term erosion. These estimates of erosion are of the order of 0.01 mm/yr to 0.1 mm/yr and correspond to time scales of roughly 10^5 yr. Based on theory derived from censored measurements of rate distributions, the short-term rates can be used to infer expected long-term rates. In this case, distributions of measured and expected long-term rates do not overlap, and an explicit test of a null hypothesis is not necessary. We interpret the large-magnitude, short-time-scale rates as a product of recent influences on the ravines, and we discuss how this framework could be applied in other settings.

INTRODUCTION

Earth science literature contains an abundance of studies describing time-dependent rates of fluvial incision (Mills, 2000; Reusser et al., 2004; Pederson et al., 2006; Wegmann and Pazzaglia, 2009), landscape denudation (Nott and Roberts, 1996; Shuster et al., 2005; Gomez et al., 2007; Moon et al., 2011), and rock uplift (Huntington et al., 2006; Blythe et al., 2007; Miller et al., 2013). Cases have been described in which modern rates are greater than (Mills, 2000; Peizhen et al., 2001; Wegmann and Pazzaglia, 2002; Hewawasam et al., 2003; Reusser et al., 2004; Huntington et al., 2006), less than (Kirchner et al., 2001; Ferrier et al., 2005; Vanacker et al., 2007; Gabet et al., 2008), and similar to (Gunnell, 1998; Campbell and Church, 2003; O'Farrell et al., 2007; Cyr and Granger, 2008) rates associated with longer time scales. Process rate changes like these are a primary method for deducing the consequences of environmental change through Earth history. For instance, changes in rates of vertical motions of rocks and surfaces have been interpreted as past tectonic changes (Reiners et al., 2002) and as the effects of Quaternary climate changes on erosion rates (Peizhen et al., 2001).

Understanding and predicting the consequences of climate variability, tectonic variation, and direct human influence on Earth's surface and environmental evolution are two of the many important modern topics in earth science that could and should be addressed by measuring temporal variation in rates of surface change. Much work has already been done to identify and quantify the effects of human action and climate alteration on the processes that erode, transport, and deposit sediment across continental surfaces. These studies include the general geomorphic influence of human action (Knox, 1977; Hooke, 2000; Douglas and Lawson, 2000; Hewawasam et al., 2003; Wilkinson and McElroy, 2007; Reusser et al., 2015), global agricultural impacts on landscapes and the environment (Nearing et al., 2000; Van Oost et al., 2005, 2007), effects of surface-water impoundments on sediment accumulation (Vörösmarty et al., 2003; Syvitski et al., 2005; Snyder et al., 2006; Yang et al., 2007; Dai et al., 2008), and direct and indirect enhancements of coastal geomorphic processes (Mazda et al., 2002; Day et al., 2007; McNamara and Werner, 2008). A major societal responsibility of earth scientists must be to define the range of possible surface behaviors under background conditions so that modern deviations from geologically normal behavior can be accurately determined and properly ascribed to anthropogenic and/or natural changes in environmental forcing (e.g., climatic, tectonic, or biologic factors).

Quantifying surface change with methods that integrate over time scales longer than any possible anthropogenic forcing is one approach that can be used to establish metrics for background geomorphic behavior. These measures

†bmcelroy@uwyo.edu

GSA Bulletin; https://doi.org/10.1130/B31644.1; 12 figures.

can then be compared against results from analyses using methods that integrate over years to decades or centuries. In order to accurately assess the significance of any observed difference, it is imperative to know the effects of integration over disparate time scales on a set of measurable surface changes. For this reason, we set out to explore a null hypothesis for analyzing rates of surface change through time and its implications and applications to data sets on rate changes.

Knowledge Gap and Problem Statement

More than three decades ago, Sadler (1981) recognized that the lack of completeness of the stratigraphic record in fluvial and other largely depositional environments could affect how rates of geologic processes appear. He demonstrated empirically and numerically that rates of deposition explicitly depend on the duration of geologic time represented by that rate (Sadler, 1981). This phenomenon seems to be explained physically by the presence of hiatuses or other variations in deposition regardless of their character as periodic or stochastic (Sadler, 1981; Schumer et al., 2011). Gardner et al. (1987) also recognized this phenomenon for a wide variety of largely erosional systems. Recently, Finnegan et al. (2014) and Gallen et al. (2015) specifically identified causative factors (erosional hiatuses and choice of datum, respectively) for erosion rate dependence on measurement interval in bedrock incision. Additionally, Ganti et al. (2016) illustrated how glaciated regions also show erosion rate dependence on time scale. These results demonstrate that regardless of the net behavior of evolving topography and ignoring potential bias or censoring, fluctuations between erosion and deposition result in time-scale dependence of rates of change for a surface. We incorporate this notion into a schematic model of surface behavior in order to generate a null hypothesis for rates of surface change.

Despite the frequent occurrence of interpretations of environmental changes based on measured differences in rates of topographic evolution, evaluations of null hypotheses to confirm the significance of these differences are seldom carried out. This is not particularly surprising because there is currently a vigorous debate about the existence of evidence showing that time-scale rate dependence exists in any meaningful way (Herman and Champagnac, 2016; Willenbring and Jerolmack, 2016). A reasonable path forward to resolve this issue must include a clear demonstration of time-scale dependence in a single location, and it must produce a consistent framework for addressing the time-scale dependence of surface process rate changes.

General Strategy to Address Problem

We address this here by analyzing the expected evolutionary behavior and history of surface topography at a single location with minimal assumptions. First, the problem is defined, and a generalized null hypothesis for topographic evolution is presented. Then, the application of probability theory to the analysis of topographic change data is described, and data from a growing channel network located in Florida, United States, are analyzed within this framework.

To accomplish this, we examined the schematic history of topographic evolution of an idealized surface. Given the previous arguments, the direction of net change of the surface does not matter when investigating the time-scale dependence of rates. However, for clarity and because the example data set used herein is from an eroding landscape, we will describe our schematic surface as undergoing net erosion. The key point is that the idealized net change (erosion) is not constant but contains fluctuations about a central behavior.

The questions of primary interest in this system are: What is the apparent time-scale dependence of erosion rate? Can it be distinguished from erosion rate changes induced by changes in the system's boundary conditions imposed from fluctuating tectonic or climatic forcing mechanisms? In order to answer this question, we needed to develop a null hypothesis for time-scale dependence of erosion rate in the absence of mean rate changes through time.

THEORY

In order to proceed with a null hypothesis, the physical system must first be fully defined. Earth's surface is subject to a great range of sedimentary and geomorphic processes. Plate tectonics and mantle dynamics control substantial vertical motions of the crust (Fowler, 1990), and differences between vertical motions of surfaces and the crustal rocks beneath capture the essential result of erosion (Molnar and England, 1990) and depositional preservation (Wilkinson et al., 2009). In many ways, these are two sides of the same coin, but they are rarely treated as such. Intermittent deposition is known in largely erosional systems. Common examples are transient alluvial (Ouimet et al., 2007) or glacial (Straumann and Korup, 2009) sediment storage in mountain valleys or transient storage of hillslope sediment associated with vegetation (DiBiase and Lamb, 2013). Similarly, intermittent erosion in largely depositional systems has long been held as the source of stratal boundaries (Krumbein and Sloss, 1963) and as a partial explanation for the lack of complete evolutionary suites of preserved paleontological organisms (Darwin, 1859).

An important aspect to consider is that surface evolution on Earth proceeds with substantial variability. Whether the variability represents a process that could be predicted with appropriate data is not particularly important. Neither is it imperative that a stochastic model of Earth's surface be adopted. Rather, the critical point is that the variability in Earth surface processes must be embraced in any reasonable null hypothesis.

In addition to the importance of process variability, it must be recognized that there is a minimum interval of time associated with meaningful evaluation of erosion rates. For example, in sandy systems undergoing relatively fast rates of denudation, e.g., 1 mm/yr, this rate is equal to the removal of no more than approximately ten grains per year at any location. For systems where physical erosion dominates mass loss from the surface, granularity limits the shortest possible scales of temporal continuity. In the example of 1 mm/yr, the shortest possible time scale of continuity is on the order of a month. For systems eroding more slowly, the shortest scales must be longer in proportion to the grain size and inversely proportional to the erosion rate. This defines a fundamental time scale below which an erosion rate has no physical meaning. The existence of this time scale is directly connected to the granularity of landscapes and is here termed the granularity time scale, T_g.

$$T_g = D_{50}\varepsilon^{-1}, \tag{1}$$

where D_{50} is the median diameter of clasts being removed from the surface, and ε is the erosion rate of the surface. Consider that it is not possible to physically denude a landscape at a rate of 0.5 grains per year over the course of a single year. At a minimum, that rate is only physically possible at a time scale of 1 grain/0.5 grains per year = 2 yr or greater.

Null Hypothesis for Surface Change

The simplest null hypothesis for an eroding landscape is no change in the rate of the erosional processes, ε.

$$\varepsilon(t) = C. \tag{2}$$

Here, erosion rate is a constant function, C, of time, t, only and is presented in one dimension. This null hypothesis (Eq. 2) could be applied across all landscapes, and at any specific locale, it could be interpreted as no change in the style

or magnitude of topographic evolution. Unfortunately, a key factor renders this particular null hypothesis inapplicable: measurement error.

This issue can be addressed by modifying the null hypothesis statement to one of no measurable change in the rate of erosion processes. The importance of the phrasing "measurable change" is that any rate variation must be larger than inherent uncertainties associated with the particular method used to determine the rate. For any rate change that is smaller than methodological uncertainty, this null hypothesis would be satisfied. It is therefore possible for modest variations in topographic change to be masked if they have only small effects on the resulting measured rates. For example, if geomorphic alteration is a weak function of climate, it could be difficult to measure the effects of changes in precipitation or temperature on rates of change within the precision offered by various measurement techniques. This problem has been specifically elucidated for basin-scale rates of denudation calculated from cosmogenic radionuclide concentrations in alluvial sediment (Schaller and Ehlers, 2006).

By additionally recognizing temporal variability in rates of topographic change, the null hypothesis can allow for both deterministic uncertainty in the measurement technique and for stochasticity in the erosional processes. This new null hypothesis is mathematically symbolized as follows:

$$\langle \varepsilon \rangle_T = C, \tag{3}$$

where the brackets represent an averaging operator over an arbitrary time period, T. A factor for measurement uncertainty need not be separately included in the formulation.

An explicit framework for applying this null hypothesis (Eq. 3) can be developed by decomposing a local elevation history, $\Delta\eta$, into its mean elevation change, $\langle \Delta\eta \rangle$, and a deviatoric component representing the variability around that change, $\Delta\eta'$.

$$\Delta\eta = \langle \Delta\eta \rangle + \Delta\eta'. \tag{4}$$

Following this, the rates of elevation change in the elevation history can be analogously decomposed into a mean rate and the variations around that rate.

$$\varepsilon = \langle \varepsilon \rangle + \varepsilon'. \tag{5}$$

Through inspection of Equations 3 and 5, it is clear that the null hypothesis (Eq. 3) specifically regards the mean portion of topographic change rates (over periods greater than the granularity time scale) and not the total rate of elevation change. Through inspection of Figure 1, it is clear that fluctuations in surface evolution imply that the magnitude of the deviatoric component of surface change is a function of time in history and the time scale of investigation. As a result, it is even possible in general and in the example case to observe deposition over some time scale, T (Fig. 1), even though the deviatoric components of elevation change and erosion rate are zero by definition.

$$\sum \Delta\eta' = \sum \varepsilon' = 0. \tag{6}$$

When geoscientists measure erosion rates at a particular location, they are measuring the total erosion or total rate, i.e., the first term in Equations 4 or 5 (Fig. 1). It is therefore necessary to evaluate the contribution of the deviatoric component of topographic evolution (as defined in Eq. 4 and Eq. 5) to any measured erosion rates before evaluating the null hypothesis (Eq. 3). In some cases, the difference between the mean and total erosion could be small, and no accounting for the difference is necessary because the associated error is small. However, in cases where the variability in erosion rate is large relative to the mean rate, the distinction between mean, $\langle \varepsilon \rangle$, and total erosion rates, ε, is no longer trivial and must be accounted for. Under these circumstances, it becomes necessary to deconvolve the mean and variable portions of the total measured erosion rate.

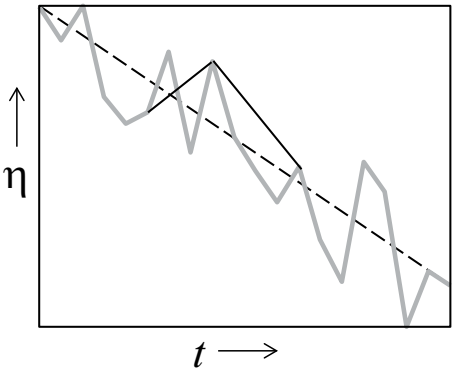

Figure 1. Schematic surface change history (Eq. 4). Thick gray curve represents a history of elevations showing mean erosion, $\langle \eta \rangle < 0$ (thin dashed line), through time and variability, $\Delta\eta'$. Slopes of thin black cords represent erosion rates, ε, at times spanned by the cords. Note that, depending on the duration and temporal location of a cord, its slope (and erosion rate) can be greater than, less than, or approximately equal to the mean rate; it could even show change of the opposite sign, i.e., aggradation in this example.

Limitations to Measurement

Evaluation of variability in rates of topographic evolution requires measurement of a distribution of erosion and deposition rates for a given location. Two types of bias are ubiquitous in modern studies of erosion and deposition and substantially affect reported rates and distributions of rates. First, methodological constraints artificially limit the ranges of measurable rates through bounds on measureable time scales and/or length scales. Second, most geomorphic and sedimentologic studies specifically set out to study rates of erosion or deposition alone, but seldom both, even though evidence for both surface aggradation and degradation is simultaneously present in most landscapes. By focusing on one direction of surface change, the other is normally excluded, leading to a measured distribution of surface changes that is a truncated version of the total surface change distribution (Fig. 2A).

Various methods have been used in surface process studies to determine ages of surfaces and buried materials as well as the affiliated rates of erosion or deposition. Physically based methods, such as the dendrogeomorphic methods applied in this study, are limited to relatively small length scales, i.e., centimeters, by imprecision associated with the response of vegetation to minor amounts of soil burial or excavation. Similarly, other methods that require vertical change estimation are often limited by resolvable change levels that are direct functions of measurement instrumentation. Further, uncertainty in creating and comparing digital elevation models introduces another host of limits to change detection (Wheaton et al., 2010). As a whole, these limits to small-scale elevation changes constrain a lower bound on achievable rates (Fig. 2B; Anders et al., 1987). This type of rate limit is independent of any time-scale–dependent rate limit that is implied by granularity.

In a similar vein, natural systems are likely to have physical constraints that place upper limits on their achievable vertical changes. For example, the Caspian Basin is likely Earth's deepest sedimentary basin at 20–25 km (Brunet et al., 2003). It is therefore an approximation of the largest achievable thickness of sediment accumulation. This provides a constraint for vertical change and for vertical change rates achievable for natural systems (Fig. 2B; Anders et al., 1987). The mathematical expression for upper and lower bounds to vertical changes is given by:

$$\Delta\eta_{min} < \Delta\eta_m < \Delta\eta_{max}, \tag{7}$$

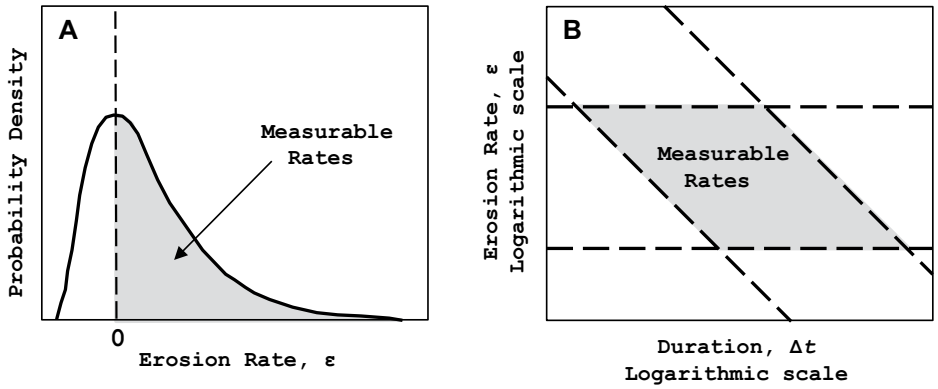

Figure 2. Schematic representation of measurable rates (Eq. 7, Eq. 8, and Eq. 9). (A) Measurable rates are often truncated by bias such that rates of the other sign are not measured in the field. The applicable types of limits vary from case to case. (B) In general, every measurement technique has limitations that set bounds on what rates are measureable. Horizontal dashed lines are limits on rates themselves, for instance, from chemical saturation or detection limits. Inclined dashed lines are limits on measurable length scales, including resolution of a ruler or potentially limits on the system such as grain-scale change or uplift/subsidence limits.

where $\Delta\eta_{max}$ and $\Delta\eta_{min}$ are the maximum and minimum measurable surface topographic changes, respectively, and $\Delta\eta_m$ is the measureable change.

Another type of constraint analogous to Equation 7 based on rates of change must also be explored. For instance, geochemically based methods are often limited by saturation of a chemical concentration in a material or by minimal concentrations required for detection. For example, radiocarbon techniques can generally date materials younger than 50–60 ka (Trumbore, 2000), a practical age-dating range for $^{230}Th/^{234}U$ system is 5–300 ka (Ku, 2000), and ^{210}Pb is only applicable to sediment deposits younger than 250 yr (Noller, 2000). Rates of erosion based on accumulation of cosmogenic nuclides are a direct function of the nuclide half-lives and are limited in a practical sense to a range between 10^0 mm/yr to 10^{-4} mm/yr (Fig. 2B; Lal, 1988). The mathematical expression for this type of rate limit is given by:

$$\varepsilon_{min} < \varepsilon_m < \varepsilon_{max}. \quad (8)$$

Here, ε_{min} and ε_{max} are the minimum and maximum measureable topographic rate changes, respectively, and ε_m is the measurable rate. Like Equation 7, Equation 8 describes a type of bias that is inherent in physical systems or the methods we employ to study them. This bias is unavoidable but largely understood.

Another type of bias is censorship connected to study design. One of the consequences of specifically attempting to measure erosion rates is that all localities within a study area that have undergone recent aggradation are by definition excluded. Naturally, for techniques that require costly analysis, there is no value in collecting samples that will yield nothing to measure. The effect of censorship is to truncate the distribution of real, local elevation change rates to a set of measureable erosion rates with shared direction of change, e.g., exclusively erosion (Fig. 2A). The mathematical expression for censorship of rates is given by:

$$\frac{\varepsilon_m}{|\varepsilon_m|} = \frac{\langle\varepsilon\rangle}{|\langle\varepsilon\rangle|} = \frac{\varepsilon'}{|\varepsilon'|}. \quad (9)$$

Equation 9 describes a common condition where the sign of the values for the measurable rate is the same as that for the real mean rate and the real deviatoric component of the rate; i.e., mean erosion is not measured at a locality of recent or net deposition. Although this is not a strict condition on measurement methods, when true, it has profound implications for measurable rates.

In a probability context, the truncation of natural distributions through the mechanism summarized in Equation 9 results in the collection of conditional rate distributions that answer the question, "What is the distribution of topographic change rates given that erosion occurred?" This question is equivalent to asking, "What is the distribution of erosion rates?" However, it is not equivalent to asking the question, "What is the distribution of topographic change rates?" The latter is the question that must be addressed in order to assess the null hypothesis in Equation 3, specifically because fluctuations in deposition and erosion are ubiquitous, and deviatoric components of surface change must be evaluated.

Because the fluctuating portions of surface change can be encapsulated in essence by a random walk of the topographic surface, and because random walks have a rich literature and theoretical development, we investigated random walks as a source of intuition about the behavior of surface changes.

Random Walks of Topography

There are many varieties of random walks with respect to their mathematical description (Feller, 1966). Here, a discreet topographic random walk is specifically defined by:

$$\eta_{t+\Delta t} = \eta_t + \Delta\eta, \quad (10)$$

where the values of $\Delta\eta$ are independent and identically distributed surface changes. Additionally, the durations between topographic changes, Δt, are constrained to be independent and identically distributed. The behavior of Equation 10 is well known for distributions of $\Delta\eta$ and Δt where the mean, $\langle\Delta\eta\rangle$, and variance, σ_η^2, are defined (Bouchaud and Georges, 1990; Weeks and Swinney, 1998; Schumer et al., 2009). In practical terms, this implies that the mean and variance do not continue to grow if more measurements are made. Originally termed Brownian motion for the case where the variance grows linearly with time, this kind of random walk taken by an ensemble of walkers gives rise to normal diffusion (Feller, 1966). If, however, the mean and variance are not constrained (e.g., because either of the distributions are heavy-tailed), then the process gives rise to anomalous diffusion (Bouchaud and Georges, 1990; Weeks and Swinney, 1998; Schumer et al., 2009).

In order to connect discrete random walks of Earth surface topography to the null hypothesis (Eq. 3), we define their behavior through time in four parts, the mean and variance of topographic change, $\Delta\eta$, and the mean and variance of a rate, ε. First, the mean component of change is found as:

$$\langle\Delta\eta\rangle = \frac{1}{N}\sum\Delta\eta, \quad (11)$$

where N is the number time steps, Δt, that were made. The variance of topographic changes, σ_η^2, gives a description of the average departures of the surface from mean changes. For normal diffusion, this is written

$$\sigma_{\Delta\eta}^2 = 2\delta N\Delta t, \quad (12)$$

where δ is a term representing the dispersive tendencies of the process of topographic change, and it is quantified as:

$$\delta = \frac{\langle \Delta\eta^2 \rangle - \langle \Delta\eta \rangle^2}{2\Delta t}. \quad (13)$$

For a surface that experienced such evolution, and that was queried with censorship given by Equations 7 and 9, the expected elevation of the surface after one step would be approximated by

$$\Delta\eta = \langle \Delta\eta \rangle + \sqrt{\sigma^2_{\Delta\eta}}. \quad (14)$$

Compare this to Equation 4.

The mean component of the rate of topographic change associated with this random walk is given by

$$\langle \varepsilon \rangle = \frac{1}{T} \sum \Delta\eta, \quad (15)$$

where T is total duration of topographic evolution equal to

$$T = \sum_N \Delta t. \quad (16)$$

The variance of the rate is related to the variance of the topographic steps (Eq. 12) by

$$\sigma^2_\varepsilon = \frac{1}{T^2} \sigma^2_{\Delta\eta}. \quad (17)$$

Finally, the expected rate of topographic change from a random walk sampled with censorship is given by

$$\varepsilon = \langle \varepsilon \rangle + \sqrt{\frac{2\delta}{\Delta t}}. \quad (18)$$

The implications of Equation 18 applied to the null hypothesis (Eq. 3) are as follows. First, if geoscientists who attempt to measure histories of surface change apply methods with censorship, then their estimates of rate changes necessarily include a component that reflects the system's variability around long-term mean change. Second, this censorship effect is more pronounced at short time scales and diminishes for most types of variability at long time scales. Third, the null hypothesis of changes in mean rates, ⟨ε⟩, can only be evaluated if an estimate of system variability at short time scales can be assessed. In other words, a distribution of rates of change is necessary to constrain this problem.

The second effect points to an important difference between actual distributions and measureable distributions of rates of surface change. For a set of measureable rates constrained by Equations 7, 8, and 9, the differences between the real behavior of a random walk and its measurable representation are not trivial. If the real distribution of rates of topographic change is truncated through censorship, then the measurable mean rate of change appears to be a function of time at short time scales, even though the uncensored distribution of change has a constant average regardless of time scale (Fig. 3). Only at longer time scales does the measurable mean appear to coincide with the real mean. This effect results from the distribution of real rates, ε, narrowing over time through natural integration processes. Effectively, the mechanism of censorship diminishes as the distribution of rates narrows at greater time scales (Fig. 3).

Crossover Time Scale

Inspection of Equation 18 and Figure 3 gives rise to the question, "At what time scale will the effect of censorship diminish?" Equivalently, when does the mean rate of a censored distribution begin to approach the mean rate of the uncensored distribution? The answer can be deduced directly from Equation 18. Setting the squared ratio of the mean erosion rate and the erosion variability to unity defines a time scale at which the two components are equal.

$$\Delta t = \frac{2\delta}{\langle \varepsilon \rangle^2}. \quad (19)$$

This is termed the crossover time scale. It is the time scale over which short-term variability gives way to long-term mean behavior as the dominant control on rates measured from a censored distribution. At shorter time scales, one should expect to see a large influence of process variability in rate measurements. At longer time scales, one should expect to see diminished effects of process variability in rate measurements.

FIELD SITE

We applied the theory laid out in the previous section to a growing channel network draining from the Tallahassee Hills into the Apalachicola River north of Bristol, Florida, United States (Fig. 4). Within the Apalachicola Bluffs and Ravines Preserve, Beaverdam Creek drains a few tens of square kilometers of upland area by groundwater seepage (Fig. 4B). Stratigraphic exposures along the adjacent Alum Bluff and within the channel network display a relatively homogeneous stratigraphy. The channel network is incised into a 65-m-thick section of laterally ungraded, medium to coarse sand deposited in fluvio-deltaic and coastal marine settings during the late Pliocene to Pleistocene (Schmidt, 1983). Some reworking of the surface in the Holocene has also been suggested (Schmidt, 1985; Rupert, 1991). These sands, with minor gravel, silt, and mud, were derived from erosion of the southernmost Appalachians and were likely deposited during progradation and stasis of the Apalachicola delta associated

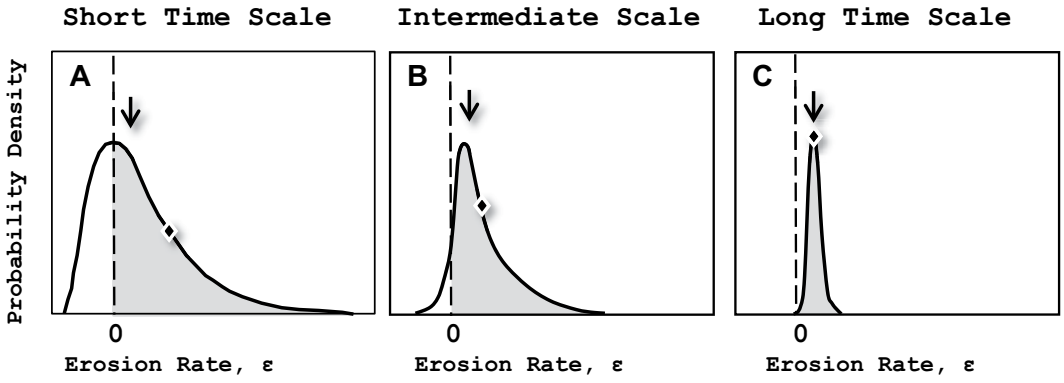

Figure 3. Effects of censorship on apparent rates of surface change from (A) short time scales to (C) long time scales. At short time scales, much of the distribution of rates can be censored, and as a result, the mean of the measureable rates (black diamond with white outline) is greater than the mean of the entire distribution (black arrow). As the process of surface change continues, many realizations of the short-term process are incorporated into local records of change, and the real and measurable rates become closer (B) until finally they are equal (C) when the process has gone on long enough that censoring no longer occurs.

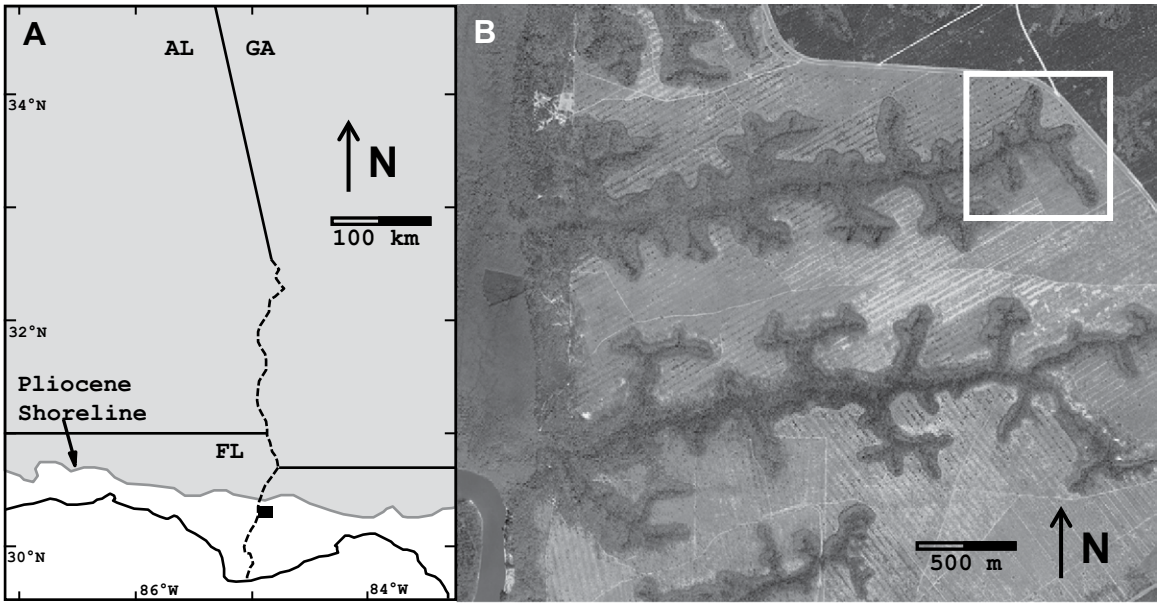

Figure 4. (A) Regional map showing ancient shoreline and a portion of the modern position of Apalachicola River (black dashed line). Black square is location of the field site. FL—Florida; AL—Alabama; GA—Georgia. (B) Orthorectified aerial photograph of Apalachicola Bluffs and Ravines Nature Preserve. White box outlines the upper Beaverdam Creek study locale (Fig. 6). The Apalachicola River and Alum Bluff are present in the lower left corner.

mainly with Pleistocene interglacial sea-level highstands (Schmidt, 1983). At Alum Bluff, these sediments unconformably overlie 15 m of muddy Miocene marine carbonates and sands (Schmidt, 1985). Greater detail of the late Neogene history of the Apalachicola region is unknown because of the nonfossiliferous nature of these sandy units (Isphording and Flowers, 1983; Schmidt, 1983).

At the upper Beaverdam Creek site, flat uplands are nearly barren of large, woody vegetation as a result of discontinued agroforestry, and they do not support overland flow because of high infiltration rates (up to 12 in./hr or 35 cm/hr; Schumm et al., 1995). Excavation at spring locations indicated no obvious stratigraphic control on their vertical positions. This observation was also reported by Schumm et al. (1995) for nearby regions.

Upper Beaverdam Creek is incised into the Pliocene–Pleistocene strata at slopes near repose to typical depths of 20 m to 25 m, with some as deep as 30 m (Fig. 5). Valley depths typically range from 20 m to 25 m, with some as deep as 30 m. Valley widths range from 20 m to 200 m and are typically 80 m to 100 m. Valley bottoms are generally flat with widths around 10 m and in the range of 1 m to 30 m. The typical channel geometry has a roughly 1 m^2 cross section with a depth of 0.5 m and a width of 2 m. This presents a rather small width to depth ratio, but thalweg depths are normally 0.1 m or less. In some cases, thalweg depths approach 1 m deep where cascades or woody debris have initiated bed scours. These conditions persist with very little hydrographic variation. Even during a strong rainfall event in January 2007, we observed no significant flow increase and no overland flow.

Valley head and valley bottom slopes were determined from a profile extracted along the valley axis from a light detection and ranging (LiDAR) digital elevation model. Valley head slopes are very near the angle of repose for noncohesive sand (30°–35°; Fig. 5). Trees are the most abundant vegetation on the slopes, but they do not appear to affect slope magnitudes. Although they would seem to add cohesion to the sediment, thus increasing the slopes, they also cause tree throw, which increases the net downhill flux, thus reducing the slopes. While both of these effects can be found locally, they possibly offset each other in net effect on longer time scales.

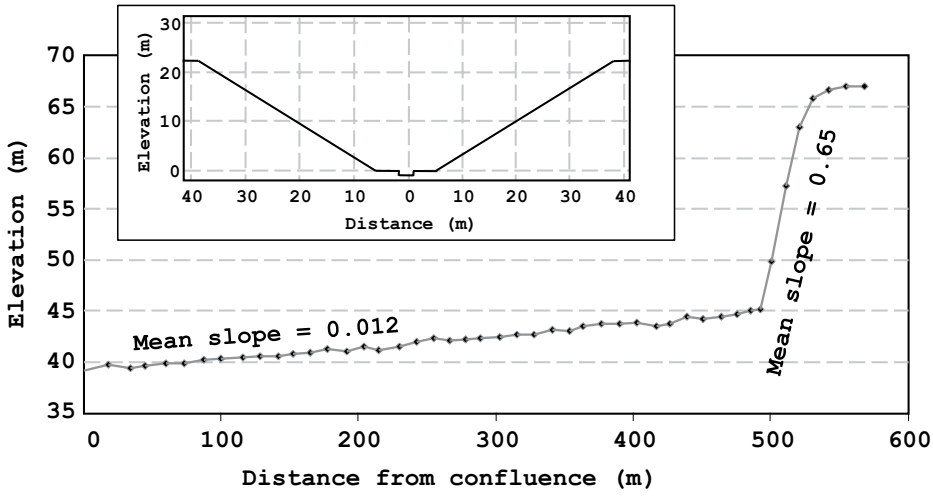

Figure 5. Longitudinal profile of valley bottom and valley head of uppermost 500 m of Beaverdam Creek showing mean slopes of valley head and valley floor. Valley head slope is near the angle of repose for sand. (Inset) Typical valley cross section showing valley bottom width ~10 m, channel width ~2 m and depth ~0.5 m, and valley depth ~20–25 m.

The vegetation that covers the valley floors and walls is an integral part of the sediment transport system; directly, tree throw moves mass, and indirectly, fallen branches, living roots, and tree trunks can accelerate or decelerate fluid flow in the channel, altering its local ability to transport sediment. In this context, it is easy to imagine feedbacks and dynamic behaviors among vegetation growth, channel migration, and surface erosion.

During the aggregate field work period, no signs of anthropogenic influences on the geomorphology of the bluffs and ravines were observed. There is a ditch at the upstream end of one branch of Beaverdam Creek (Fig. 6, segment D). However, even during very heavy rain, infiltration rates were high enough to inhibit overland flow in the ditch. It was built to allow easy access to water at the spring. Additionally, and also because infiltration rates are so high, we concluded that logging of the upland surface is also unlikely to have dramatically changed the geomorphology of the system over human time scales.

METHODS

To better understand the behavior of this growing channel network, we made estimates of erosion rate from measurements of total erosion and erosion duration in the upper reaches of Beaverdam Creek using dendrogeomorphic methods. These methods are ideal for this system because it is possible to gather hundreds of erosion rates that average over time scales of decades to centuries. Additionally, cosmogenic nuclide geochemical methods were applied in an attempt to determine rates at time scales of tens of thousands of years. These two methods are detailed next.

Dendrogeomorphic Methods

We considered the growth of trees in Beaverdam Creek to be an integral part of the process that evolves the valley bottom topography. In this context, the position in space of the tree roots adjacent to their associated tree trunks was taken as an indicator of the elevation of the surface under which they initially grew. Distances between the modern surface and living tree roots were interpreted to represent vertical changes in position of the valley surface through time—either burial through deposition or exposure through erosion (Fig. 7). The net rate of topographic change was then determined by the ratio of burial or exposure distance, $\Delta\eta$, to tree age, Δt. This approach uses the age of the tree as a surrogate for the duration of the root's existence.

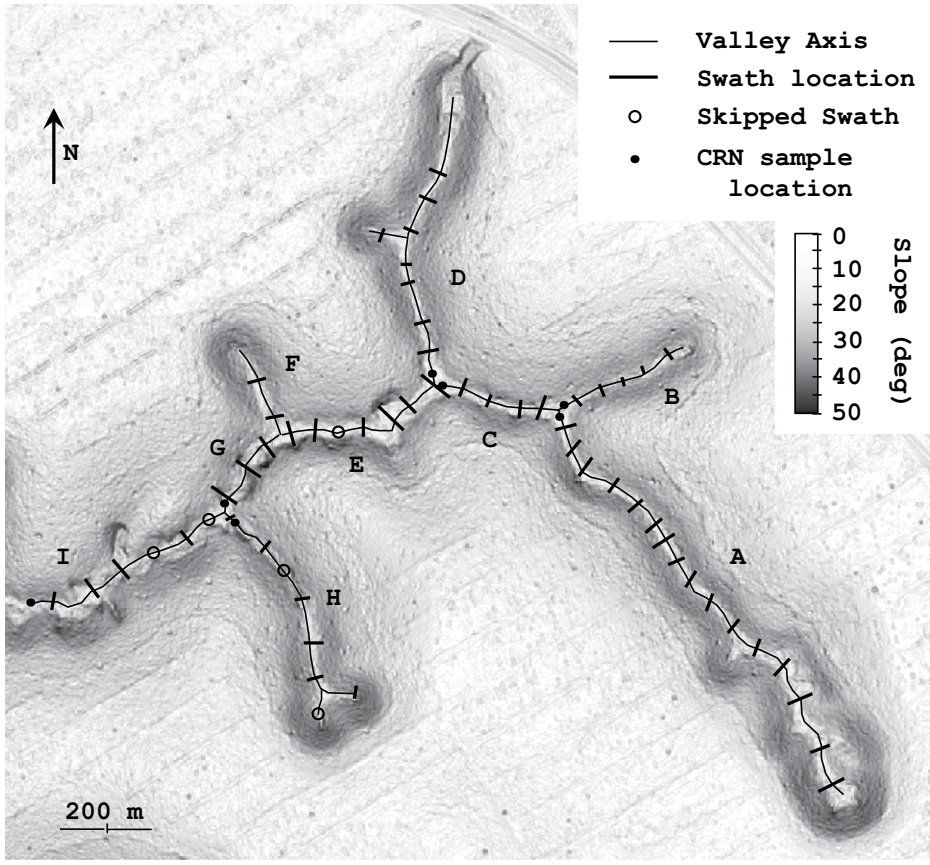

Figure 6. Map of upper Beaverdam Creek showing locations of dendrogeomorphic sampling swaths (thick black lines) and locations where channel sands were sampled for cosmogenic radionuclide (CRN) analysis (filled black circles). Grayscale represents the magnitude of local slope. Channel segments are labeled with capital letters, and CRN samples are located at the downstream end of each segment. CRN samples share labels with the segment from which they were collected (e.g., reach A and CRN sample A-01). The skipped swaths (open black circles) contained no standing trees larger than 2 in. (5 cm) in diameter. The longitudinal profile of segment A is shown in Figure 5.

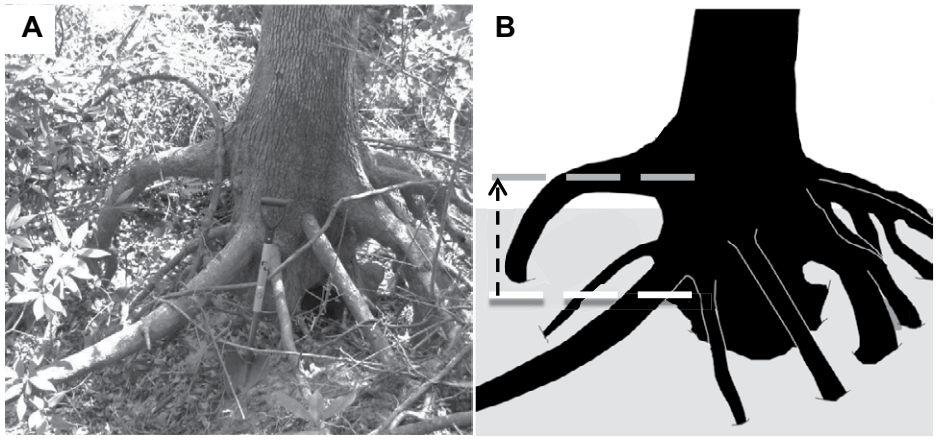

Figure 7. (A) Photograph of example tree with roots exposed by erosion. (B) Schematic representation of tree in photo showing example interpretation of surface elevation at the time of tree germination. White dashed line gives position of modern sediment surface. Gray dashed line shows interpreted pregrowth surface. Black dashed line represents vertical separation of modern and pregrowth surfaces used to estimate erosional thickness, $\Delta\eta$, over life span of tree, Δt.

Not every root is equally useful as a paleosurface indicator. For each measured tree, a best root was chosen based on its quality relative to other roots. Of the roots exposed adjacent to each tree, the highest subhorizontal root was judged to be the most likely indicator of the elevation of the soil surface at the inception of tree growth. This procedure does not systematically select the greatest eroded thickness or the greatest erosion rate because the modern ground surface is neither planar nor likely to be parallel to the paleosurface. Additionally, measurements were taken of elevation change at locations where tree roots crossed over the modern, active channel. Provided that roots of the trees sampled do not initiate growth above the soil or channel bottom surface, the highest root is an indication of the lowest possible position of the surface when that root started to grow. Because roots do not necessarily grow in a radially symmetric pattern, the actual position of an original root relative to its mature position is known to a precision of about half of a root diameter. Therefore, the center position of each root was used, and a nominal, vertical positioning error of 0.05 m was adopted. This positioning error was estimated based on a characteristic root size. Root exposure heights that measured less than 0.05 m were within this minimum confidence window and were therefore taken to be zero. This ensured that small vertical differences associated with roots exposing themselves by growing upward through the soil surface were not taken as evidence of erosion.

Tree ages used as proxies for the initiation of root growth at adjacent positions were determined by two methods. Over the entire field site, cores were collected at breast height (~1.5 m) from 33 trees with a 5.15 mm Haglof increment borer, and the annual growth rings were counted under a binocular microscope. The number of growth rings indicates the time since the tree reached breast height and not since its germination. For the tree species under consideration, the time for a tree to grow to breast height would generally be on the order of a few years and is ignored because this accrued error is small compared to the uncertainty associated with the timing of root growth and its position relative to the soil surface. For the other 330 trees used to make estimates of topographic change, a relation between trunk diameter at breast height, D_{bh}, and tree age was constructed (Eq. 20; Fig. 8).

Tree ages and diameters are geometrically related by the function

$$Age\ (\mathrm{yr}) = 4.8\ (\mathrm{yr/cm}) \times D_{bh}^{0.85}\ (\mathrm{cm}). \quad (20)$$

This relation includes trees of four species: *Fagus grandifolia*, *Magnolia grandiflora*, *Quercus alba*, and *Pinus glabra*. Traditionally, dendrochronologic studies make single-species age-diameter relations to exclude interspecies variation in growth rates through tree ontogeny. In this case, these four species compose the large majority of codominant tree species in the canopy of the Apalachicola ravines (Kwit et al., 1998). Because they have similar stature in the canopy and share practically identical environmental conditions on the valley floors, growth rates of these four species are similar enough to make a single age-diameter relation. This is evident from the high degree of correlation of *Age* with D_{bh}: for the entire collection, the Pearson correlation coefficient is 0.83, and the standard error of the age estimates is 0.15 logarithmic units (i.e., ~1–40 yr across the age spectrum of 7–200 yr).

One third of the trees that were cored were chosen for excellent examples of root exposure such as a very clearly defined paleosurface or spectacularly large eroded thicknesses. The rest of the trees that were cored came from two randomly selected valley bottom transects. All trees within these two transects were sampled. The oldest tree cored was a 198-yr-old *Quercus alba* with a breast-height diameter of 37.6 cm. The youngest tree cored was a 7-yr-old *Fagus grandifolia* with a breast height diameter of 2.0 cm. This range of diameters nearly brackets the entire distribution of tree diameters measured, and therefore the distribution of calculated ages is largely interpolated, leaving little excess error in the tree age estimates from extrapolation.

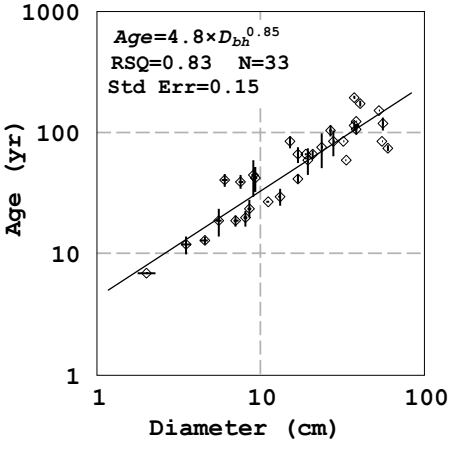

Figure 8. Age-diameter plot for 33 trees collected from valley floor of upper Beaverdam Creek. Vertical and horizontal black bars show error range estimates for each tree's age and diameter, respectively. Four tree species are included: *Pinus glabra*, *Magnolia grandiflora*, *Fagus grandifolia*, and *Quercus alba*. Pearson correlation coefficient is R^2 (RSQ) = 0.83 for N = 33 samples with a standard error of the age estimate = 0.15 log units. D_{bh}—diameter of tree at breast height.

In order to calculate dendrogeomorphic erosion rates, best ages were estimated for all trees. For those trees that were cored, the best age estimate was the number of annual rings counted from the core. For those trees that were not cored, best ages were estimated by applying the age-diameter relation to each measured diameter. Error in cored trees was approximated during inspection of the cores, and for calculated ages, the age error was estimated from the standard error of the age estimate given by the age-diameter relation, 0.15 log units. These best ages represent the duration, Δt, over which the valley bottom topography has evolved adjacent to the tree during root growth.

In and along the margins of upper Beaverdam Creek, 381 root exposures were measured in a total of 59 swaths (Fig. 6). Each swath occupied 10 m of along-valley distance, covered the entire valley width, and was separated by a distance of 30 m between their centers. This represents a sampling of approximately one third of all trees covering the 4 km of valley bottom length. Of these swaths, only five had no measurable or live standing trees larger than 2 in. (5 cm) in diameter at breast height. In one case, the valley width was only a few meters, and the channel occupied the entire width, and in three of the other cases, large trees had fallen and apparently took all nearby, smaller trees down with them. The largest swath was 28.0 m across and contained 14 trees with measurable root exposure; the narrowest swath was 3.5 m across and contained seven trees with measurable root exposure. The number of root exposures measured per swath ranged between 2 and 22. The number of roots measured can be greater than the number of trees measured because in some instances single trees had roots exposed over the valley bottom as well as channel-spanning roots. In these cases, both were measured. In total, this collection represents a sampling of positions along the valley bottom that is as uniform and as unbiased as possible, and it includes eroding, unchanging, and aggrading areas of the growing channel network.

Cosmogenic Methods

The accumulation of cosmogenic radionuclides in materials near the surface of eroding landscapes has been used to make estimates

of basin-averaged erosion rates (Bierman and Steig, 1996; Granger et al., 1996). Brown et al. (1995), Granger et al. (1996), and Biermann and Steig (1996) proposed that sediments in channels represent a mixed sample from the eroding hillslopes of the basins that they drain. With the appropriate caveats, von Blankenburg (2006) summarized this idea as the "let nature do the averaging" approach. In this context, we collected sand samples from the modern channel bottom at seven locations in the upper Beaverdam Creek channel network (Fig. 6). Sampling sites were located directly above each of the major confluences as well as at the farthest downstream valley bottom swath.

Sand particles composing these samples were moderately well sorted, had a median diameter of 0.45 mm, and were predominantly quartz. Beryllium extraction was performed at the University of Minnesota cosmogenic laboratory between April and May of 2007. The chemical blank ratio (^{10}Be/^{9}Be) run with this sample was 6×10^{-15}, thus 9.34×10^{4} atoms of ^{10}Be were added with the chemical blank. The quartz sample was spiked with 250 µl of a 10^{-3} g/g ^{9}Be solution from Centre de Recherche en Sciences de Gestion (CEREGE), Aix-en-Provence, France, before dissolution. An adaption of the Kohl and Nishiizumi (1992) chemical procedure was used for quartz purification and Be extraction. The ratio of cosmogenic to native (carrier-added) Be was measured via Acceleratory Mass Spectrometry (AMS) at PRIME Laboratory at Purdue University during June and July of 2007.

In addition to the fluvial sand samples, two other samples were gathered from the field area: a soil sample from the upland surface labeled S-01, and a sample buried underneath the soil profile at the same location, labeled S-02. In order to get a measure of surface deflation rate or age of the upland, the upland surface sample was taken at a position outside the area of hillslope curvature but within the ravine forest. Positions outside the ravine forest have been disturbed historically by timber harvesting. The buried sample was taken from a vertical position ~5 m below the upland surface underneath the surface sample by excavating into a near-vertical wall within a valley head. The valley head lacked vegetation, but authigenic kaolinite was present and appeared to be adding the cohesion necessary to make a nearly vertical face. These features were taken to indicate relatively rapid erosion. Sand was sampled from the back of a small hole at ~0.7 m into the valley head face, and its ^{10}Be concentration should approximate the inherited concentration of ^{10}Be accumulated in the deltaic sediments prior to burial during the latest Pliocene to earliest Pleistocene.

RESULTS

Dendrogeomorphic

Total erosion was determined for each exposure site by measuring the thickness of soil or channel substrate excavated since growth of tree roots. Of those, 128 indicated total topographic change less than the minimum confidence thickness of 0.05 m and were reported as zero. Thicknesses eroded for the remaining 253 exposures ranged from 0.05 m to 1.37 m. For these 253 measurements, total erosion, $\Delta\eta$, integrated over the duration of the tree lives, Δt, is an increasing function of tree age described by a power function (Fig. 9) with a Pearson correlation coefficient of 0.28.

$$\Delta\eta\ (\mathrm{m}) = 0.013\ (\mathrm{m/yr}) \times \Delta t^{0.54}\ (\mathrm{yr}). \quad (21)$$

Nonerosion values (no change or aggradation) cannot be plotted in logarithmic space, but they can be included implicitly by applying a 10 yr averaging window to the data. The running average then includes the zero values and can be plotted in logarithmic space. The best-fit power function for the ensemble averaged total erosion has a Pearson correlation coefficient of 0.69.

$$\Delta\eta\ (\mathrm{m}) = 0.0014\ (\mathrm{m/yr}) \times \Delta t^{1.05}\ (\mathrm{yr}). \quad (22)$$

From inspection of Figure 9, it is clear that the variability of total erosion on the valley bottom increases as a function of erosion duration. Naturally, small trees do not have deep enough roots to allow them to record very fast erosion. To make a quantitative evaluation, the variance of the total erosion, $\sigma^2_{\Delta\eta}$, was calculated in six bins across the range of durations. The bins were delimited in duration increments that roughly equalized the size of the bins while maintaining a minimum number of ~30 measurements per bin: <30 yr, 30–50 yr, 50–70 yr, 70–90 yr, 90–110 yr, >110 yr. With a Pearson correlation coefficient of 0.97, Figure 10 demonstrates a linear relation between variance of total erosion, $\sigma^2_{\Delta\eta}$, and erosion duration, or best tree age. This is given by

$$\sigma^2_{\Delta\eta}\ (\mathrm{m}^2) = 0.00013\ (\mathrm{m}^2/\mathrm{yr})\ \Delta t\ (\mathrm{yr}). \quad (23)$$

Dendrogeomorphic erosion rates, ε, were calculated by dividing the total erosion thicknesses, $\Delta\eta$, by the erosion duration, Δt. Erosion rates, ε, ranged from 0.3 mm/yr upwards to 16.8 mm/yr. These rates are inversely related to the erosion duration (Fig. 9). This correlation is imposed by the length scale limit, below which erosion rate cannot be measured, and by an apparent upper limit to erosion rates across scales. Because the data for this relation are the exact same as those in Figure 9, correlation of erosion rate to duration is equivalent to that of total ero-

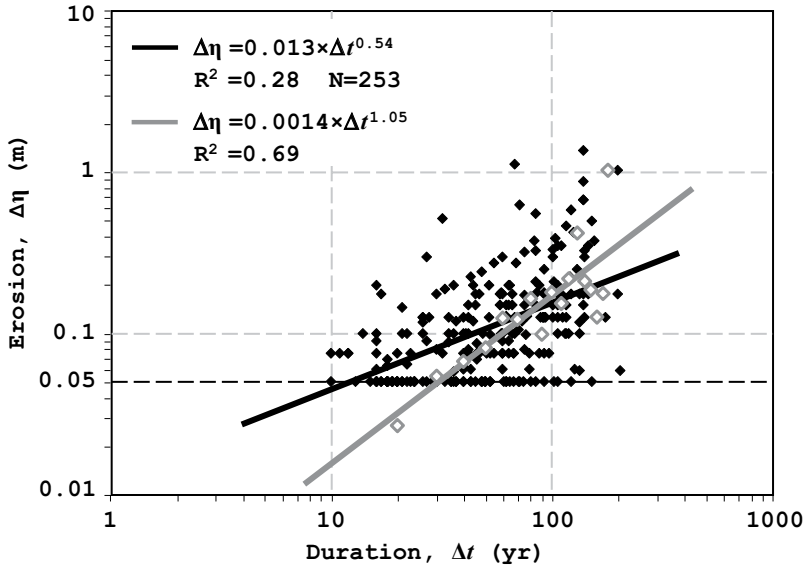

Figure 9. Total erosion, $\Delta\eta$, as a function of erosion duration, Δt. Solid black diamonds are original dendrogeomorphic data excluding $\Delta\eta = 0$, because those data cannot be plotted in logarithmic space. White diamonds with black outline are 10 yr window averages of $\Delta\eta$, including all zero values. Black dashed line is the cutoff level for measurement, 0.05 m. Black solid line is best fit to the original data (Eq. 21). Gray line is best fit to windowed averages (Eq. 22) that include 128 measurements of zero erosion.

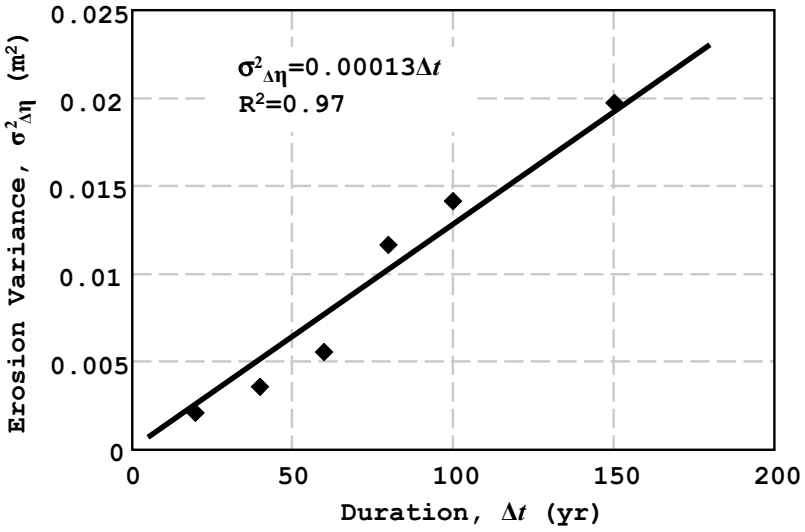

Figure 10. Variance of total erosion, $\sigma^2_{\Delta\eta}$, as a function of erosion duration, Δt (Eq. 23). Variance was calculated for measurements of total erosion grouped into six bins and exhibits a linear dependence on duration.

sion and duration. The relation from Equation 21 can be transformed into a fit for Figure 11 by subtracting one from the exponent of Δt; this has the effect of dividing by Δt.

$$\varepsilon\ (\text{m/yr}) = 0.013\ (\text{m/yr}^2) \times \Delta t^{-0.46}\ (\text{yr}). \quad (24)$$

Inclusion of all the nonerosion (zero) rates was accomplished by using the same 10 yr window average that was used to create running average dendrogeomorphic erosion thicknesses (Fig. 9). Once the zero values were included, it became clear that erosion rates had no correlation with duration of topographic evolution (Pearson correlation coefficient of 0.004).

$$\varepsilon\ (\text{m/yr}) = 0.0014\ (\text{m/yr}^2) \times \Delta t^{0.05}\ (\text{yr}). \quad (25)$$

Cosmogenic Nuclides

Concentrations of ^{10}Be measured from the upland surface, buried sands, and active fluvial sands varied between 2.90×10^5 atoms/g and 4.10×10^5 atoms/g. The buried sand sample, labeled S-01, has been shielded from recent accumulation of radionuclides and defines an inherited concentration of 9.86×10^4 atoms/g. Assuming that the inheritance is equivalent for all samples, the concentration of sample S-01 was subtracted from concentrations of all other samples in order to determine modern ^{10}Be accumulation. The accuracy of these values is evident from their internal consistency within the channel network. Each sample collected downstream of a confluence should have a concentration intermediate between the two contributing upstream reaches. This is true for all sample sets from Beaverdam Creek: B-01 < C-01 < A-01, D-01 < G-01 < C-01, and G-01 < I-01 < H-01. In general, the uncertainties are on the order of <5% of concentration values, which range from 1.91×10^5 to 3.11×10^5 atoms/g.

Using the CRONUS-Earth online calculator (Balco et al., 2008), an erosion rate was estimated for the upland surface from the depth-shielding–corrected S-02 sample concentration. Input values for latitude, longitude, and elevation were 30.49°N, 84.95°W, and 50 m, respectively. This sample comes from the forested part of the upland with existing tree throws, and therefore mixing of the soil profile to modest depths is expected on time scales of the lives of trees. The sample thickness was estimated to be 30 cm due to this mixing. Sample density was measured in the field and is 1.3 g/cm^3. There was no topographic shielding on the upland, and the CRONUS-Earth calculation standard used was KNSTD07. For the range of assumptions given in the calculation method (Balco et al., 2008), erosion rate estimates varied between 0.015 mm/yr and 0.016 mm/yr, with uncertainties between 0.0012 mm/yr and 0.0015 mm/yr. The upland area appears to be eroding at a rate of ~0.01 mm/yr.

DISCUSSION

Dendrogeomorphic Data, Censorship, and Erosion Rate Distributions

The dendrogeomorphic method was used to generate a data set in which the effects of censorship on a distribution of erosion rates could

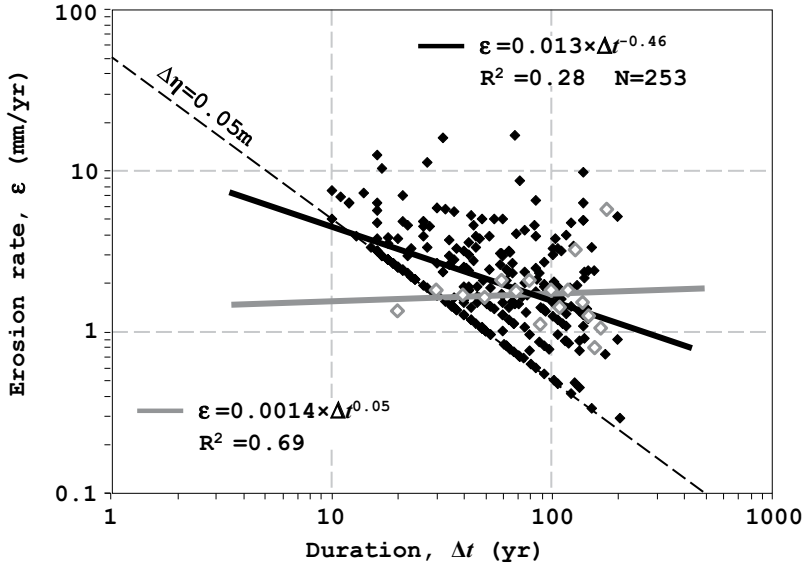

Figure 11. Erosion rate, ε, as a function of duration, Δt. Solid black diamonds are original dendrogeomorphic data excluding $\Delta\eta = 0$, because those data cannot be plotted in logarithmic space. White diamonds with gray outline are 10 yr window averages of $\Delta\eta$, including all zero values. Black dashed line marks the cutoff level for measurement, 0.05 m. Black solid line is the best fit to the original data (Eq. 24). Gray line is best fit to the window-averaged data that include $\Delta\eta = 0$ (Eq. 25). This indicates no correlation between rate and duration when the entire distribution of surface change is included.

be directly explored. Beaverdam Creek and the surrounding ravines are incising, and their steepheads are retreating at relatively high rates on the order of 1 mm/yr (Abrams et al., 2009), and there is little evidence of deposition in the channel network. However, there are many locations that appear to have experienced no topographic change over the life spans of living trees. As a result, the complete data set includes 128 measurements of zero-valued erosion rates. When these are ignored and censored out of the distribution of surface change rates (Eq. 9), the rates then exhibit time-scale dependence (Fig. 11; Eq. 24). However, when they are incorporated into the distributions of rates, then the mean behavior of the modern erosional processes at the time scales of decades to centuries is immediately recoverable (Fig. 11; Eq. 25).

The nature of the time-scale dependence of erosion rates is explicitly a function of the time-scale dependence of erosion variability in the system. The range of possible vertical erosion distances in upper Beaverdam Creek clearly increases as a function of erosion duration (Fig. 9). The evolution of the valley bottom also appears to be constrained by a maximum likely observable rate, ε_{max}, on the order of 10 mm/yr (Fig. 11). Insofar as the data are constrained between a maximum rate (Eq. 8) and the minimum observable length scale (Eq. 7), and measurements fill the space in between, the variance must be an increasing function of duration. In Beaverdam Creek, erosion variance of the surface as measured by tree root exposure grows linearly with time (Fig. 10; Eq. 23). Linear growth of variance is a hallmark of normal diffusion (Feller, 1966). In this case, substituting Equation 12 into Equation 18 gives the expected inverse square-root time-scale dependence of rates in a normal diffusion process, $\varepsilon \sim \Delta t^{-0.5}$. Indeed, that is our interpretation. The ensemble of modern erosion processes in Beaverdam Creek can be modeled well by normal diffusion. Applying Equation 18 to understand the time-scale dependence of erosion rates does not require an assumption of normal diffusion. Because we were able to measure the functional form of time-scale dependence of erosion variance, we were able to apply it to Equation 18. In general, a measurement of erosion variance (i.e., a distribution of erosion rates) is required to close this problem. In cases where the landscape is best characterized by a subdiffusive process, $\sigma^2_{\Delta\eta} \sim \Delta t^{0<\gamma<1}$, short time-scale erosion rates should scale as $\varepsilon \sim \Delta t^{-0.5>\beta>-1}$. Similarly, for a superdiffusive process, the variance or erosion would scale as $\sigma^2_{\Delta\eta} \sim \Delta t^{1<\gamma<2}$, and short time-scale erosion rates would scale with time as $\varepsilon \sim \Delta t^{0>\beta>-0.5}$. We applied this expected long-term behavior to help evaluate the null hypothesis (see section "Estimating Rate Changes").

Cosmogenic Erosion Rates

The suite of concentrations of ^{10}Be measured in the channel sand samples has relatively low measurement errors and complete internal consistency within the channel network. This gives confidence in their results. The erosion rates that were calculated from these data are on the order 0.01 mm/yr. Time scales associated with these rates were determined by erosion rate, the decay rate of ^{10}Be, and its absorption mean free path, and they cluster around 5×10^4 yr, about the time it takes to erode through 0.7 m of the surface. Because the time scales are inversely proportional to the rate (Lal, 1991), the plot of rate against time scale has a slope of –1 in logarithmic space (Fig. 12, gray circles).

This can be given context by estimating the time it would take to form Beaverdam Creek from this erosion rate. With a depth of ~22 m, and a mean rate of 0.013 mm/yr, the total formation time of Beaverdam Creek would be 1.7×10^6 yr. This is consistent with the Pliocene–Pleistocene age of the sediments that make up the substrate. It is approximately a factor of two larger than the total age of the system estimated by Abrams et al. (2009). Given the level of uncertainties, this difference does not seem significant enough to warrant further investigation.

Very little evidence exists on the upland surface for erosion by overland flow. However, some topographic features on the regional upland surface, the Tallahassee Hills, have been interpreted as evidence of eolian sediment transport (Schumm et al., 1995). These small hummocks and parallel topographic lineations are also present in the Ravines and Bluffs Preserve area. Therefore, the ^{10}Be concentration of the upland might be representative of a modest rate of surface deflation.

Erosion rates results give estimates of 0.016 ± 0.0014 mm/yr. For the modal grain size of 0.45 mm, the resulting erosion rate for the upland surface is ~1 grain every 30 yr; the granular time scale, T_g, is 30 yr. Taking the model age of the upper Beaverdam Creek portion of the channel network of ca. 400 ka (Abrams et al., 2009), the eolian deflation of the upland surface surrounding upper Beaverdam Creek since its inception could be on the scale of meters.

These rate estimates have uncertainty that cannot be fully quantified if upper Beaverdam Creek is not in a condition of cosmogenic steady state. This is likely to be the case because erosion is largely focused at the valley heads. The important point is whether the transport of sediment through the channel system takes longer than the period it spends on the hillslope ac-

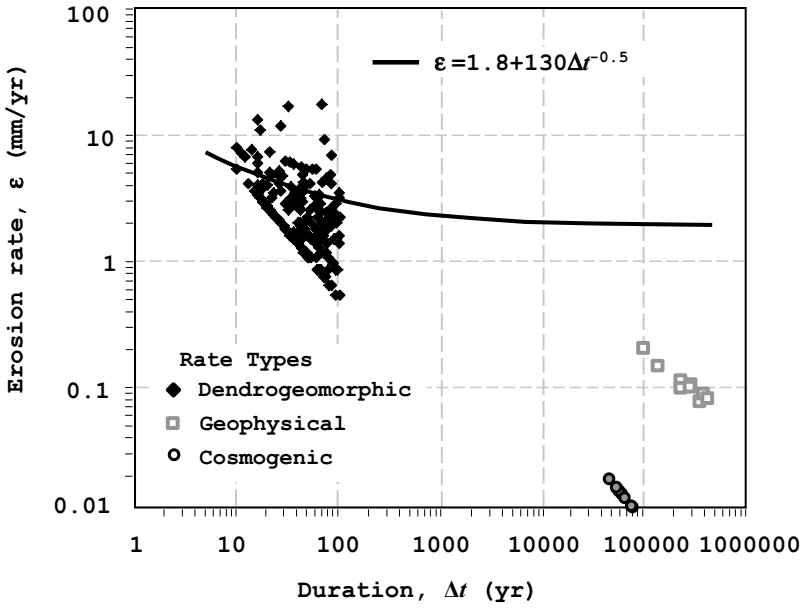

Figure 12. Comparison of erosion rates determined from three different methods, dendrogeomorphic (black diamonds), geophysical modeling (gray outlined squares), and cosmogenic (gray circles with black outlines). The solid black curve represents the best model for measurable erosion rate as a function of time scale. The vertical distance between the black curve and the population of long-term rates represents the best estimate of rate changes over the time scales of interest.

cumulating cosmogenic nuclides, or similarly if in situ–produced cosmogenic ^{10}Be is largely exported at rates equivalent to the rates at which it is produced. Cosmogenic steady state is a required assumption in the "let nature do the averaging" technique (von Blanckenburg, 2006), and therefore basin-average cosmogenic erosion rates may not be completely faithful measures of direct surface change in upper Beaverdam Creek.

Estimating Rate Changes

Secular rate changes should always be investigated in the framework of a null hypothesis. Here, we describe a null hypothesis in which measurable, average rates of change are constant (Eq.3). Primarily, for systems in which the variability of topographic change at short time scales is large relative to the mean behavior, measurable rates of change converge at relatively long time scales to the mean of the process, and the measurable mean rate is negatively correlated with evolution duration. This prediction is valid even for evolving localities where the general null hypothesis (Eq. 3) is satisfied, i.e., with zero net change. The key is in the distinction between measurable changes and the distribution of real, natural changes. These predictions are qualitatively evaluated next based on data collected in the Beaverdam Creek field site.

Because we could not ascertain in the field the complete up-and-down (deposition-and-erosion) history of a single point, we characterize the entire ensemble of trees as representative of potential changes that may have occurred within the history of any one site. The assumption is that the current distribution of observable rates and behaviors across the landscape is equivalent to the distribution of observable rates and behaviors at any single location within that landscape. This is a slightly more strict assumption than ergodicity of the erosion process alone (i.e., equivalence of time and space averaging).

One of the predictions derived from a censored distribution of topographic change is that at long time scales, the measurable erosion rates converge to the real mean of the process of topographic evolution. At short time scales, the censoring that is associated with conditions given in Equations 7, 8, and 9 is very effective at removing any aggradational periods or regions from the data set of measurable erosion rates. In contrast, erosion rates that integrate over longer periods of the history of change implicitly contain more intermediate periods of aggradation or nonerosion. The longest time-scale behavior shows that all real rates meet the conditions of measurability and therefore accurately reflect the real mean rate (Fig. 3). This behavior is not explicitly obvious in the upper Beaverdam Creek field site. Dendrogeomorphic rates were not sampled over a long enough time scale to appear to converge. Convergence toward the complete distribution at long time scales can happen at time scales much longer than the approach to mean behavior (Anders et al., 1987).

We now evaluate the null hypothesis (Eq. 3) in Beaverdam Creek as an example. In order to do this, the mean and variability of the system must be determined as related in Equation 18. Because we were able to measure an uncensored distribution of topographic change, the average estimate of erosion rate is not a function of time (Eq. 25; Fig. 11). Therefore, the value for the mean erosion rate of the modern process, $\langle \varepsilon \rangle$, was determined from the arithmetic mean of all erosion rates to be 1.8 mm/yr. This is the rate of erosion that one would expect to measure if they could do so at arbitrarily long time scales. For this reason, it is the rate that must be compared to rate estimates from methods for which sampling time scales are longer. We evaluated two sets of rates from long time scales, one from the cosmogenic measurements described here, and a second from an existing model of the evolution of Beaverdam Creek (Abrams et al., 2009).

Based on a model for the dynamics of the groundwater–surface-water system, Abrams et al. (2009) presented the age and history of the entire Beaverdam Creek (ca. 730 ka, marine oxygen isotope stage [MIS] 18; Lisiecki and Raymo, 2005), including the complete temporal evolution of the geographic position of each of the valley heads. This model offers a long-term geomorphic evolution with which to compare the short time-scale evolution measured in the field with dendrogeomorphic methods. The rates based on the Abrams et al. (2009) model were determined by comparing current valley depth to the time at which each branch of the modern network began forming. The range of rates spans 0.08–0.2 mm/yr at time scales of $1–4 \times 10^5$ yr (Fig. 12). These appear to make a group with a slope of –1 in log-log space along a contour of 20 m, the average modern channel depth.

The two sets of long-term erosion rates (model history and cosmogenic) are disparate by most of an order of magnitude and have time-scale ranges that are barely non-overlapping. The real uncertainties for each method are largely unknown. For this reason, the mean values of rates and time scales of each group were averaged in order to make a best estimate for the actual long time-scale erosion rate in Beaverdam Creek. The estimate is 0.06 mm/yr at 2×10^5 yr.

Although we could attempt a formal hypothesis test of the null hypothesis to determine the probability that the short time-scale erosion rate, 1.8 mm/yr, is different from the long time-scale erosion rate, 0.06 mm/yr, it is clear that this is not necessary. The two estimates are separated by an order and a half of magnitude, they are generated from non-overlapping populations, and inspection of Figure 12 is enough to make this point clear. In general, however, a formal test is likely to be required. In this case, we can clearly conclude that the modern processes eroding Beaverdam Creek have accelerated relative to their Quaternary history.

Crossover Time Scale

In order to determine the crossover time scale in Beaverdam Creek, we applied the mean erosion rate of the uncensored distribution, 1.8 mm/yr, and the short-term erosion variance, 130 mm^2/yr. The result is an estimate of 40 yr. This estimate fits well with our understanding of the system; it is approximately the median tree age of 43 yr. Because trees appear to be intimately involved in the processes of surface evolution, it is very reasonable that their age distribution is imprinted on the surface's evolution. Additionally, 40 yr is very close to the granularity time scale for the long-term rates. For this reason, it is not possible to directly compare dendrogeomorphic erosion rates at the scale of a few decades to the long-term rates. This is because the long-term rates simply cannot be measured at the dendrogeomorphic time scales. Only above time scales of granularity (and the crossover) do measured erosion rate differences approach real differences in surface change through time.

Evolution of Beaverdam Creek

It is apparent that rates of erosion in Beaverdam Creek have increased since the original excavation of the ravine network from the upland surface. There are two nonexclusive alternatives that could explain the observed mean erosion rate differences through time. First, modern land-use changes have been substantial in the Apalachicola Bluffs and Ravines Preserve. Prior to becoming a nature preserve, the land had been a site of agroforestry. For decades, the site was variably stripped of trees on the upland surface. As a result, infiltration of precipitation could have been enhanced over the period of recent timber operations. However, no specific data exist to quantify potential capture rates by the community of plants that would have existed prior to the land-use change. Regardless, the ultimate result of an increase in infiltration rates would be greater fluxes of water through the steephead springs, and greater rates of network evolution (e.g., Abrams et al., 2009).

Changes in precipitation through time would cause variations in infiltration rates and discharge of groundwater at springs. Laîné et al. (2009) reported that glacial-interglacial or even millennial-scale climate fluctuations, including precipitation, could have been substantial. This is also supported by local and regional palynology in the eastern United States (Grimm et al., 1993; Jackson et al., 2000), as well as regional speleothem records (Alvarez Zarikian et al., 2005; Van Beynen et al., 2008). As a result of Quaternary fluctuations in rainfall, total groundwater discharge is likely to have decreased during glacial periods, causing intermittent reduction in rates of erosion and migration of valley steepheads. Altogether, this is suggestive of a scenario in which quiescence during glacial periods was punctuated by more rapid evolution during interglacial periods. Although this explanation is far from certain, we find it more straightforward than the host of other nonunique regional histories that could lead to the modern geomorphic conditions. We therefore interpret the modern high erosion rates as likely resulting from the current interglacial condition, although it is possible that latent anthropogenic effects are convolved with natural effects of Quaternary climate variability.

CONCLUSIONS

Understanding the impact that humans have had on Earth's surface in a geomorphic sense requires collecting and comparing rates of processes across a wide range of time scales—from geologic background time scales down to the time scales of years and decades. This undertaking requires an understanding of the effects of measuring implicitly integrated surface change processes over disparate time scales. To that extent, a null hypothesis for surface evolution was presented. The evolutionary history of a location can be broken into mean and deviatoric components of elevation change (Eq. 4 and Eq. 5). The deviatoric component of the process must sum to zero (Eq. 6), and the generalized null hypothesis is that the mean rate of topographic change is temporally invariant (Eq. 3). Coupling this null hypothesis with censorship based on measurement and study design techniques (Eq. 7, Eq. 8, and Eq. 9) leads to a nontrivial time-scale dependence of measurable erosion rates.

Additionally, the following qualitative predictions are derived from the theory presented here. (1) Measurable erosion has greater variability at longer time scales than at shorter time scales and places a first-order control on time-scale dependence of erosion rates. (2) At short time scales, measurable erosion rates are negatively correlated with duration of evolution. (3) At long time scales, measurable erosion rates converge on the mean rate. (4) For rates measured at short time scales, biasing based on Equations 7, 8, and 9 effectively censors out nonerosion. In contrast at very long time scales, aggradation is implicitly integrated into the measurable rates, and the biasing condition is less effective (to ineffective) at censoring out parts of the distribution of real rates. (5) In order to evaluate the null hypothesis of no change in mean erosion rate, an estimate of erosion variance must be made. This accounts for the effect described in point 4.

The upper Beaverdam Creek field site in Apalachicola Bluffs and Ravines Preserve, Florida, United States, provides abundant opportunities to measure topographic change with dendrogeomorphic methods on the valley floor. Tree root exposure was used to determine erosion based on the distance between roots and the modern channel or soil surface. The ages of the trees are indicators of the duration over which surface processes exhumed the exposed roots. Unexposed tree roots were taken as indicators of surface stability over tree life spans. Strong and dynamic interactions between the transport of sand eroded from the relatively homogeneous sandy strata and the growing vegetation cause large variability in annual to centennial erosion rates. At short time scales, this variance increases linearly with the duration of topographic evolution (Eq. 23; Fig. 10). The process recorded here is appropriately interpreted as normal diffusion. The censored dendrogeomorphic data also demonstrate a negative correlation between erosion rate and duration (Eq. 21; Fig. 9). However, this dependence does not exist when the full distribution of topographic change is queried (Eq. 22; Fig. 9). In this case, when nonerosion is included, there is no dependence of erosion rate on the duration of topographic evolution.

Samples of alluvial sand were collected to analyze in situ–produced ^{10}Be in quartz, which measures the long-term erosion rate in a landscape at or near cosmogenic steady state. These were coupled with rates from a geophysical model of the system. Together, they suggest that the modern erosion rates are more than an order of magnitude greater than Quaternary rates. This includes an accounting for the variability required for the null hypothesis (Eq. 3 and Eq. 18).

One of the implications for this work is that studies that attempt to measure topographic change over differing time scales must be sensitive not to exclude local areas in which the sense of topographic change is opposite to the long-term trend. This exclusion will necessarily result in a negative correlation between rates and their associated time scales. This is especially true in systems where the short-term variability is large relative to the long-term trends. Furthermore, this effect must be treated appropriately in order to compare long time-scale rates to short time-scale rates for the purposes of identifying human-induced accelerations of Earth surface change.

ACKNOWLEDGMENTS

This work benefited greatly from support and discussions with D. Rothman. The manuscript was also improved by reviews and editing from V. Ganti, L. Scuderi, and K. Wegmann. We thank The Nature Conservancy and D. Printiss for access and guidance to the Apalachicola Bluffs and Ravines Preserve. Partial funding was provided by the University of Wyoming School of Energy Resources and the National Center for Earth-Surface Dynamics, a Science and Technology Center of the U.S. National Science Foundation (EAR-0203296).

REFERENCES CITED

Abrams, D., Lobkovvsky, A., Petroff, A., Straub, K., McElroy, B., Mohrig, D., Kudrolli, A., and Rothman, D., 2009, Growth laws for channel networks incised by groundwater flow: Nature Geoscience, v. 2, p. 193–196, doi:10.1038/ngeo432.

Alvarez Zarikian, C.A., Swart, P.K., Gifford, J.A., and Blackwelder, P.L., 2005, Holocene paleohydrology of Little Salt Spring, Florida, based on ostracod assemblages and stable isotopes: Palaeogeography, Palaeoclimatology, Palaeoecology, v. 225, p. 134–156, doi:10.1016/j.palaeo.2004.01.023.

Anders, M., Krueger, S., and Sadler, P., 1987, A new look at sedimentation rates and the completeness of the stratigraphic record: The Journal of Geology, v. 95, p. 1–14, doi:10.1086/629103.

Balco, G., Stone, J., Lifton, N., and Dunai, T., 2008, A simple, internally consistent, and easily accessible means of calculating surface exposure ages and erosion rates from Be-10 and Al-26 measurements: Quaternary Geochronology, v. 3, p. 174–195, doi:10.1016/j.quageo.2007.12.001.

Bierman, P., and Steig, E., 1996, Estimating rates of denudation and sediment transport using cosmogenic isotope abundances in sediment: Earth Surface Processes and Landforms, v. 21, p. 125–139, doi:10.1002/(SICI)1096-9837(199602)21:2<125::AID-ESP511>3.0.CO;2-8.

Blythe, A., Burbank, D., Carter, A., Schmidt, K., and Putkonen, J., 2007, Plio-Quaternary exhumation history of the central Nepalese Himalaya: 1. Apatite and zircon fission track and apatite [U-Th]/He analyses: Tectonics, v. 26, TC3002, doi:10.1029/2006TC001990.

Bouchaud, J., and Georges, A., 1990, Anomalous diffusion in disordered media: Statistical mechanisms, models and physical applications: Physics Reports, v. 195, p. 127–293, doi:10.1016/0370-1573(90)90099-N.

Brown, E.T., Stallard, R.F., Larsen, M.C., Raisbeck, G.M., and Yiou, F., 1995, Denudation rates determined from the accumulation of *in situ*-produced ^{10}Be in the Luquillo Experimental Forest Puerto Rico: Earth and Planetary Science Letters, v. 129, p. 193–202.

Brunet, M.F., Korotaev, M.V., Ershov, A.V., and Nikishin, A.M., 2003, The South Caspian Basin: A review of its evolution from subsidence modelling: Sedimentary Geology, v. 156, no. 1-4, p. 119–148, doi:10.1016/S0037-0738(02)00285-3.

Campbell, D., and Church, M., 2003, Reconnaissance sediment budgets for Lynn Valley, British Columbia: Holocene and contemporary time scales: Canadian Journal of Earth Sciences, v. 40, p. 701–713, doi:10.1139/e03-012.

Cyr, A., and Granger, D., 2008, Dynamic equilibrium among erosion, river incision and coastal uplift in the Northern Apennines, Italy: Geology, v. 36, p. 103–106, doi:10.1130/G24003A.1.

Dai, S., Yang, S., and Cai, A., 2008, Impacts of dams on the sediment flux of the Pearl River, southern China: Catena, v. 76, p. 36–43, doi:10.1016/j.catena.2008.08.004.

Darwin, C., 1859, On the Origin of Species by Means of Natural Selection: London, Murray, 502 p.

Day, J.W., Jr., Boesch, D.F., Clairain, E.J., Kemp, G.P., Laska, S.B., Mitsch, W.J., Orth, K., Mashriqui, H., Reed, D.R., Shabman, L., Simenstad, C.A., Streever, B.J., Twilley, R.R., Watson, C.C., Wells, J.T., and Whigham, D.F., 2007, Restoration of the Mississippi Delta: Lessons from Hurricanes Katrina and Rita: Science, v. 315, p. 1679–1684, doi:10.1126/science.1137030.

DiBiase, R.A., and Lamb, M.P., 2013, Vegetation and wildfire controls on sediment yield in bedrock landscapes: Geophysical Research Letters, v. 40, p. 1093–1097, doi:10.1002/grl.50277.

Douglas, I., and Lawson, N., 2000, The human dimensions of geomorphological work in Britain: Journal of Industrial Ecology, v. 4, p. 9–33, doi:10.1162/108819800569771.

Feller, W., 1966, An Introduction to Probability Theory and its Applications II: New York, Wiley, 626 p.

Ferrier, K., Kirchner, J., and Finkel, R., 2005, Erosion rates over millennial and decadal timescales at Caspar Creek and Redwood Creek, Northern California Coast Ranges: Earth Surface Processes and Landforms, v. 30, p. 1025–1038, doi:10.1002/esp.1260.

Finnegan, N.J., Schumer, R., and Finnegan, S., 2014, A signature of transience in bedrock river incision rates over timescales of 104–107 years: Nature, v. 505, p. 391–394, doi:10.1038/nature12913.

Fowler, C.M.R., 1990, The Solid Earth: An Introduction to Global Geophysics: Cambridge, UK, Cambridge University Press, 728 p.

Gabet, E., Burbank, D., Pratt-Sitaula, B., Putkonen, J., and Bookhagen, B., 2008, Modern erosion rates in the high Himalayas of Nepal: Earth and Planetary Science Letters, v. 267, p. 482–494, doi:10.1016/j.epsl.2007.11.059.

Gallen, S.F., Pazzaglia, F.J., Wegmann, K.W., Pederson, J.L., and Gardner, T.W., 2015, The dynamic reference frame of rivers and apparent transience in incision rates: Geology, v. 43, p. 623–626, doi:10.1130/G36692.1.

Ganti, V., von Hagke, C., Scherler, D., Lamb, M., Fischer, W., and Avouac, J., 2016, Time scale bias in erosion rates of glaciated landscapes: Science Advances, v. 2, p. E1600204, doi:10.1126/sciadv.1600204.

Gardner, T.W., Jorgensen, D.W., Shuman, C., and Lemieux, C.R., 1987, Geomorphic and tectonic process rates: Effects of measured time interval: Geology, v. 15, no. 3, p. 259–261, doi:10.1130/0091-7613(1987)15<259:GATPRE>2.0.CO;2.

Gomez, B., Carter, L., and Trustrum, N., 2007, A 2400 yr record of natural events and anthropogenic impacts in inter-correlated terrestrial and marine sediment cores; Waipaoa sedimentary system, New Zealand: Geological Society of America Bulletin, v. 119, p. 1415–1432, doi:10.1130/B25996.1.

Granger, D., Kirchner, J., and Finkel, R., 1996, Spatially averaged long-term erosion rates measured from in-situ produced cosmogenic nuclides in alluvial sediment: The Journal of Geology, v. 104, p. 249–257, doi:10.1086/629823.

Grimm, E.C., Jacobson, G.L., Jr., Watts, W.A., Hansen, B.C.S., and Maasch, K.A., 1993, A 50,000-year record of climate oscillations from Florida and its temporal correlation with the Heinrich events: Science, v. 261, p. 198–200, doi:10.1126/science.261.5118.198.

Gunnell, Y., 1998, Present, past, and potential denudation rates: Is there a link? Tentative evidence from fission-track data, river sediment loads, and terrain analysis in the South Indian shield: Geomorphology, v. 25, p. 135–153, doi:10.1016/S0169-555X(98)00026-9.

Herman, F., and Champagnac, J.D., 2016, Plio-Pleistocene increase of erosion rates in mountain belts in response to climate change: Terra Nova, v. 28, no. 1, p. 2–10, doi:10.1111/ter.12186.

Hewawasam, T., von Blanckenburg, F., Schaller, M., and Kubik, P., 2003, Increase of human over natural erosion rates in tropical highlands constrained by cosmogenic nuclides: Geology, v. 31, p. 597–600, doi:10.1130/0091-7613(2003)031<0597:IOHONE>2.0.CO;2.

Hooke, R.LeB., 2000, On the history of humans as geomorphic agents: Geology, v. 28, p. 843–846, doi:10.1130/0091-7613(2000)28<843:OTHOHA>2.0.CO;2.

Huntington, K., Blythe, A., and Hodges, K., 2006, Climate change and late Pliocene acceleration in the Himalaya: Earth and Planetary Science Letters, v. 252, p. 107–118, doi:10.1016/j.epsl.2006.09.031.

Isphording, W.C., and Flowers, G.C., 1983, Differentiation of unfossiliferous clastic sediments: Solutions from the southern portion of the Alabama–Mississippi Coastal Plain: Tulane Studies in Geology and Paleontology, v. 17, no. 3, p. 59–83.

Jackson, S.T., Webb, R.S., Anderson, K.H., Overpeck, J.T., Webb, T., III, Williams, J.W., and Hansen, B.C.S., 2000, Vegetation and environment in eastern North America during the Last Glacial Maximum: Quaternary Science Reviews, v. 19, p. 489–508, doi:10.1016/S0277-3791(99)00093-1.

Kirchner, J., Finkel, R., Riebe, C., Granger, D., Clayton, J., King, J., and Megahan, W., 2001, Mountain erosion over 10 yr, 10 k.y., and 10 m.y. time scales: Geology, v. 29, p. 591–594, doi:10.1130/0091-7613(2001)029<0591:MEOYKY>2.0.CO;2.

Knox, J., 1977, Human impacts on Wisconsin stream channels: Annals of the Association of American Geographers, v. 67, p. 323–342, doi:10.1111/j.1467-8306.1977.tb01145.x.

Kohl, C.P., and Nishiizumi, K., 1992, Chemical isolation of quartz for measurement of in-situ–produced cosmogenic nuclides: Geochimica et Cosmochimica Acta, v. 56, p. 3583–3587, doi:10.1016/0016-7037(92)90401-4.

Krumbein, W., and Sloss, L., 1963, Stratigraphy and Sedimentation: San Francisco, California, Freeman, 660 p.

Ku, T., 2000, Uranium-series methods, *in* Noller, J., Sowers, J., and Lettis, W., eds., Quaternary Geochronology Methods and Applications: American Geophysical Union Reference Shelf Volume 4, p. 101–114.

Kwit, C., Schwartz, M., Platt, W., and Geaghan, J., 1998, The distribution of tree species in steepheads of the Apalachicola River Bluffs, Florida: The Journal of the Torrey Botanical Society, v. 125, p. 309–318, doi:10.2307/2997244.

Laîné, A., Kageyama, M., Salas-Melia, D., Voldoire, A., Riviere, G., Ramstein, G., Planton, S., Tyteca, S., and Peterschmitt, J.Y., 2009, Northern Hemisphere storm tracks during the Last Glacial Maximum in the PMIP2 ocean atmosphere coupled models: Energetic study, seasonal cycle, precipitation: Climate Dynamics, v. 32, p. 593–614, doi:10.1007/s00382-008-0391-9.

Lal, D., 1988, In situ–produced cosmogenic isotopes in terrestrial rocks: Annual Review of Earth and Planetary Sciences, v. 16, p. 355–388, doi:10.1146/annurev.ea.16.050188.002035.

Lal, D., 1991, Cosmic ray labeling of erosion surfaces: In situ nuclide production rates and erosion models: Earth and Planetary Science Letters, v. 104, p. 424–439, doi:10.1016/0012-821X(91)90220-C.

Lisiecki, L.E., and Raymo, M.E., 2005, A Pliocene-Pleistocene stack of 57 globally distributed benthic $\delta^{18}O$ records: Paleoceanography, v. 20, PA1003, doi:10.1029/2004PA001071.

Mazda, Y., Magi, M., Nanao, H., Kogo, M., Miyagi, T., Kanazawa, N., and Kobashi, D., 2002, Coastal erosion due to long-term human impact on mangrove forests: Wetlands Ecology and Management, v. 10, p. 1–9, doi:10.1023/A:1014343017416.

McNamara, D., and Werner, B., 2008, Dynamics of coupled human-landscape systems: Geomorphology, v. 91, p. 393–407.

Miller, S.R., Sak, P.B., Kirby, E., and Bierman, P.R., 2013, Neogene rejuvenation of central Appalachian topography: Evidence for differential rock uplift from stream profiles and erosion rates: Earth and Planetary Science Letters, v. 369–370, p. 1–12, doi:10.1016/j.epsl.2013.04.007.

Mills, H., 2000, Apparent increasing rates of stream incision in the eastern United States during the late Cenozoic: Geology, v. 28 p. 955–957, doi:10.1130/0091-7613(2000)28<955:AIROSI>2.0.CO;2.

Molnar, P., and England, P., 1990, Late Cenozoic uplift of mountain ranges and global climate change: Chicken or egg?: Nature, v. 346, p. 29–34, doi:10.1038/346029a0.

Moon, S., Chamberlain, C.P., Blisniuk, K., Levine, N., Rood, D.H., and Hilley, G.E., 2011, Climatic control of denudation in the deglaciated landscape of the Washington Cascades: Nature Geoscience, v. 4, no. 7, p. 469–473, doi:10.1038/ngeo1159.

Nearing, M., Romkens, M., Norton, L., Stott, D., Rhoton, F., Laflen, J., Flanagan, D., Alonso, C., Bingner, R., Dabney, S., Doering, O., Huang, C., McGregor, K., and Simon, A., 2000, Measurement and models of soil loss rates: Science, v. 290, p. 1300–1301, doi:10.1126/science.290.5495.1300b.

Noller, J., 2000, Lead-210 geochronology, *in* Noller, J., Sowers, J., and Lettis, W., eds., Quaternary Geochronology Methods and Applications: American Geophysical Union Reference Shelf Volume 4, p. 115–120.

Nott, J., and Roberts, R., 1996, Time and process rates over the past 100 m.y.: A case for dramatically increased landscape denudation rates during the late Quaternary in northern Australia: Geology, v. 24, p. 883–887, doi:10.1130/0091-7613(1996)024<0883:TAPROT>2.3.CO;2.

O'Farrell, C., Heimsath, A., and Kaste, J., 2007, Quantifying hillslope erosion rates and processes for a coastal California landscape over varying timescales: Earth Surface Processes and Landforms, v. 32, p. 544–560, doi:10.1002/esp.1407.

Ouimet, W.B., Whipple, K.X., Royden, L.H., Sun, Z., and Chen, Z., 2007, The influence of large landslides on river incision in a transient landscape: Eastern margin of the Tibetan Plateau (Sichuan, China): Geological Society of America Bulletin, v. 119, no. 11-12, p. 1462–1476, doi:10.1130/B26136.1.

Pederson, J., Anders, M., Rittenhour, T., Sharp, W., Gosse, J., Karlstrom, K., 2006, Using fill terraces to understand incision rates and evolution of the Colorado River in eastern Grand Canyon, Arizona: Journal of Geophysical Research–Earth Surface, v. 111, F02003, doi:10.1029/2004JF000201.

Peizhen, Z., Molnar, P., and Downs, W., 2001, Increases in sedimentation rates and grain sizes 2–4 Myr ago due to the influence of climate change on erosion rates: Nature, v. 410, p. 891–897, doi:10.1038/35069099.

Reiners, P.W., Ehlers, T.A., Garver, J.I., Mitchell, S.G., Montgomery, D.R., Vance, J.A., and Nicolescu, S., 2002, Late Miocene exhumation and uplift of the Washington Cascade Range: Geology, v. 30, no. 9, p. 767–770, doi:10.1130/0091-7613(2002)030<0767:LMEAUO>2.0.CO;2.

Reusser, L., Bierman, P., Pavich, M., Zen, E., Larsen, J., and Finkel, R., 2004, Rapid late Pleistocene incision of Atlantic passive margin river gorges: Science, v. 305, p. 499–502, doi:10.1126/science.1097780.

Reusser, L., Bierman, P., and Rood, D., 2015, Quantifying human impacts on rates of erosion and sediment transport at a landscape scale: Geology, v. 43, p. 171–174, doi:10.1130/G36272.1.

Rupert, F., 1991, The Geomorphology and Geology of Liberty County, Florida: Florida Geological Survey Open-File Report 43, 9 p.

Sadler, P.M., 1981, Sediment accumulation rates and the completeness of stratigraphic sections: The Journal of Geology, v. 89, p. 569–584, doi:10.1086/628623.

Schaller, M., and Ehlers, T., 2006, Limits to quantifying climate driven changes in denudation rates with cosmogenic radionuclides: Earth and Planetary Science Letters, v. 248, p. 153–167, doi:10.1016/j.epsl.2006.05.027.

Schmidt, W., 1983, Neogene Stratigraphy and Geologic History, Apalachicola Embayment, Florida [Ph.D. dissertation]: Tallahassee, Florida, Florida State University, 233 p.

Schmidt, W., 1985, Alum Bluff, Liberty County, Florida: Florida Geological Survey Open-File Report 9, 11 p.

Schumer, R., Meerschaert, M., and Baeumer, B., 2009, Fractional advection-dispersion equations for modeling transport at the Earth surface: Journal of Geophysical Research–Earth Surface, v. 114, F00A07, doi:10.1029/2008JF001246.

Schumer, R., Jerolmack, D., and McElroy, B., 2011, The stratigraphic filter and bias in measurement of geologic

rates: Geophysical Research Letters, v. 38, no. 11, L11405, doi:10.1029/2011GL047118.

Schumm, S., Boyd, K., Wolff, C., and Spitz, W., 1995, A ground-water sapping landscape in the Florida Panhandle: Geomorphology, v. 12, p. 281–297, doi:10.1016/0169-555X(95)00011-S.

Shuster, D., Ehlers, T., Rusmore, M., and Farley, K., 2005, Rapid glacial erosion at 1.8 Ma revealed by $^{4}He/^{3}He$ thermochronometry: Science, v. 310, p. 1668–1670, doi:10.1126/science.1118519.

Snyder, N., Wright, S., Alpers, C., Flint, L., Holmes, C., Rubin, D., 2006, Reconstructing depositional processes and history from reservoir stratigraphy: Englebright Lake, Yuba River, northern California: Journal of Geophysical Research–Earth Surface, v. 111, F04003, doi:10.1029/2005JF000451.

Straumann, R.K., and Korup, O., 2009, Quantifying postglacial sediment storage at the mountain-belt scale: Geology, v. 37, no. 12, p. 1079–1082, doi:10.1130/G30113A.1.

Syvitski, J., Vörösmarty, C., Kettner, A., and Green, P., 2005, Impact of humans on the flux of terrestrial sediment to the global coastal ocean: Science, v. 308, p. 376–380, doi:10.1126/science.1109454.

Trumbore, S., 2000, Radiocarbon geochronology, *in* Noller, J., Sowers, J., and Lettis, W., eds., Quaternary Geochronology Methods and Applications: American Geophysical Union Reference Shelf Volume 4, p. 41–60.

Vanacker, V., von Blanckenburg, F., Hewawasam, T., and Kubik, P., 2007, Constraining landscape development of the Sri Lankan escarpment with cosmogenic nuclides in river sediment: Earth and Planetary Science Letters, v. 253, p. 402–414, doi:10.1016/j.epsl.2006.11.003.

Van Beynen, P.E., Soto, L., and Polk, J., 2008, Variable calcite deposition rates as proxy for paleo-precipitation determination as derived from speleothems in central Florida, USA: Journal of Caves and Karst Studies, v. 70, p. 25–34.

Van Oost, K., Van Muysen, W., Govers, G., Quine, T.A., and Deckers, J., 2005, From water to tillage erosion dominated landscape evolution: Geomorphology, v. 72, p. 193–203, doi:10.1016/j.geomorph.2005.05.010.

Van Oost, K., Ritchie, J., McCarty, G., Heckrath, G., Kosmas, C., Giraldez, J., Marques da Silva, J., and Merckx, R., 2007, The impact of agricultural soil erosion on the global carbon cycle: Science, v. 318, p. 626–629, doi:10.1126/science.1145724.

von Blanckenburg, F., 2006, The control mechanisms of erosion and weathering at basin scale from cosmogenic nuclides in river sediment: Earth and Planetary Science Letters, v. 237, p. 462–479, doi:10.1016/j.epsl.2005.06.030.

Vörösmarty, C., Meybeck, M., Fekete, B., Sharma, K., Green, P., and Syvitski, J., 2003, Anthropogenic sediment retention: Major global impact from registered river impoundments: Global and Planetary Change, v. 39, p. 169–190, doi:10.1016/S0921-8181(03)00023-7.

Weeks, E., and Swinney, H., 1998, Anomalous diffusion resulting from strongly asymmetric random walks: Physical Review E: Statistical Physics, Plasmas, Fluids, and Related Interdisciplinary Topics, v. 57, p. 4915–4920, doi:10.1103/PhysRevE.57.4915.

Wegmann, K., and Pazzaglia, F., 2002, Holocene strath terraces, climate change, and active tectonics: The Clearwater River basin, Olympic Peninsula, Washington State: Geological Society of America Bulletin, v. 114, p. 731–744, doi:10.1130/0016-7606(2002)114<0731:HSTCCA>2.0.CO;2.

Wegmann, K.W., and Pazzaglia, F.J., 2009, Late Quaternary fluvial terraces of the Romagna and Marche Apennines, Italy: Climatic, lithologic, and tectonic controls on terrace genesis in an active orogen: Quaternary Science Reviews, v. 28, no. 1-2, p. 137–165, doi:10.1016/j.quascirev.2008.10.006.

Wheaton, J.M., Brasington, J., Darby, S.E., and Sear, D.A., 2010, Accounting for uncertainty in DEMs from repeat topographic surveys: Improved sediment budgets: Earth Surface Processes and Landforms, v. 35, no. 2, p. 136–156.

Wilkinson, B., and McElroy, B., 2007, The impact of humans on continental erosion and sedimentation: Geological Society of America Bulletin, v. 119, p. 140–156, doi:10.1130/B25899.1.

Wilkinson, B.H., McElroy, B.J., Kesler, S.E., Peters, S.E., and Rothman, E.D., 2009, Global geologic maps are tectonic speedometers—Rates of rock cycling from area-age frequencies: Geological Society of America Bulletin, v. 121, no. 5-6, p. 760–779, doi:10.1130/B26457.1.

Willenbring, J.K., and Jerolmack, D.J., 2016, The null hypothesis: Globally steady rates of erosion, weathering fluxes and shelf sediment accumulation during late Cenozoic mountain uplift and glaciation: Terra Nova, v. 28, no. 1, p. 11–18, doi:10.1111/ter.12185.

Yang, S., Zhang, J., and Xu, X., 2007, Influence of the Three Gorges Dam on downstream delivery of sediment and its environmental implications, Yangtze River: Geophysical Research Letters, v. 34, L10401, doi:10.1029/2007GL029472.

Science Editor: Bradley S. Singer
Associate Editor: Karl W. Wegman

Manuscript Received 29 August 2016
Revised Manuscript Received 5 March 2017
Manuscript Accepted 28 June 2017

Printed in the USA